Numer. Math. Theor. Meth. Appl.
doi: 10.4208/nmtma.2014.1236nm

Vol. 7, No. 1, pp. 107-122
February 2014

A Study of Multiple Solutions for the Navier-Stokes Equations by a Finite Element Method

Huanxia Xu[1], Ping Lin[2,*] and Xinhui Si[1]

[1] *Department of Mathematics and Mechanics, University of Science and Technology Beijing, Beijing 100083, China.*
[2] *Department of Mathematics, University of Dundee, Dundee DD1 4HN, UK.*

Received 8 November 2012; Accepted (in revised version) 28 April 2013

Available online 24 January 2014

Abstract. In this paper, a finite element method is proposed to investigate multiple solutions of the Navier-Stokes equations for an unsteady, laminar, incompressible flow in a porous expanding channel. Dual or triple solutions for the fixed values of the wall suction Reynolds number R and the expansion ratio α are obtained numerically. The computed multiple solutions for the symmetric flow are validated by comparing them with approximate analytic solutions obtained by the similarity transformation and homotopy analysis method. Unlike previous works, our method deals with the Navier-Stokes equations directly and thus has no similarity and other restrictions as in previous works. Finally we use the method to study multiple solutions for three cases of the asymmetric flow (which has not been studied before using the similarity-type techniques).

AMS subject classifications: 76M10, 76D05, 74H15

Key words: Finite element method, Navier-Stokes equations, porous channel, expanding walls.

1. Introduction

In recent decades, there are growing interests in studying the laminar flow in channels or pipes with porous and expanding or contracting walls due to their relevance to a number of biological and engineering models, such as the transport of biological fluids through contracting or expanding vessels, the synchronous pulsation of porous diaphragms, the modeling of air circulation in the respiratory system and the model of the regression of the burning surface in solid rocket motors. Furthermore, the classical Berman's problem can be regarded as a special case of this model when the walls are stationary.

In order to study the transpiration cooling, Berman [1] established the model to describe the diffusion of fluids at a porous channel. He regarded Reynolds number as a small

*Corresponding author. *Email addresses:* plin@maths.dundee.ac.uk (P. Lin), xuhuanxia568@163.com (H. X. Xu), xiaoniustu@163.com (X. H. Si)

parameter and obtained the asymptotic solution for the first time. Since then a large number of analytic and numerical investigations for the problem have been done. In general, most of the researchers reduce the Navier-Stokes equations to a boundary value problem of a 4th-order nonlinear ordinary differential equation (ODE) through a similarity transformation and then obtain its asymptotic or numerical solutions. For example, Yuan [2], Terrill and Shrestha [3], Suryaprakashrao [4] obtained asymptotic solutions using perturbation method and discussed the relation between the velocity field and the Reynolds number. In the numerical investigation of the solutions of the flow (ODE) in a stationary channel, they use an initial value method to solve the boundary value problem. The shooting method combined with a Runge-Kutta integrator was mainly employed. Terrill [3,5,6] may be the earliest to have numerical studies for the laminar flow of different Reynolds number R in a porous channel and obtained one solution for a few Reynolds numbers R. Robinson [7], Lu et al. [8] and Zaturska et al. [9] discussed the multiplicity of solution for the flow of different R in a porous channel with stationary walls by numerically solving the nonlinear ODE. All of numerical studies for the similarity-transformed ODE model with stationary walls have revealed that one solution exists for $-12.165 \leq R \leq 0$ and three solutions exist for$-\infty < R < -12.165$.

However, very little has been done for the multiple solutions of the flow in a porous channel with moving walls. Majdalani and Zhou [10–13], Asghar et al. [14] and Saeed et al. [15] discussed the flow in a deforming channel using perturbation method, Adomian decomposition method (AMD) and homotopy analysis method respectively, but they did not focus on the multiplicity of the solution. Dauenhauer and Majdalani [16] believed that multiple solutions should exist for the flow in a porous channel with expanding or contracting walls and should be influenced by both R and expansion ratio α. Recently, Xu et al. [17] investigated the multiple solutions of the flow in a porous channel with moving walls using the homotopy analysis method. They obtained two new profiles that are complementary to the solutions explored by Dauenhauer and Majdalani [16].

Durlofsky and Brady [18] indicated that similarity solutions are important in helping us understand the behavior of fluids. However, there is no assurance that these solutions represent a physically realizable flow and that these solutions are physically stable. This is the motivation that we study the multiple solutions by solving the original governing Navier-Stokes equations without making a similarity transformation. Furthermore, our method based directly on the original equations may be applied to general problems without any restriction accompanied with the similarity transformation (for example, the assumption of constant expansion ratio is not necessary in our method).

In this paper, we shall directly solve the Navier-Stokes equations using the finite element method, which is a very popular numerical method for partial differential equations, especially for various fluid flow problems (see e.g., [19–21]). We aim to study the multiple solutions for the flow in a porous channel with moving walls by employing a continuous finite element method. The moving walls are converted to fixed walls through a simple variable transformation. Since we deal with the time dependent governing equations directly the dynamic stability of these solutions may be justified through the solving process. In Section 2, we introduce the model of the laminar flow in a porous channel with expand-

ing or contracting walls. In Section 3, we describe the corresponding weak formulation and the finite element method. In Section 4, the numerical results for symmetric flow are presented and validated through comparisons with approximate analytical solutions obtained in Xu et al. [17]. Then we apply the method to obtain multiple solutions of the governing equations with asymmetric boundary conditions, which have not been studied by the method of similarity transformation.

2. The governing equations

Consider the unsteady, incompressible laminar flow through a two-dimensional rectangular channel with porous walls through which the fluid is injected or extracted at an absolute velocity v_0 at the lower wall and an absolute velocity v_1 at the upper wall. As shown in Fig. 1, the distance $2a(t)$ between the porous walls is taken to be much smaller than the width and the length of the channel. A coordinate system is chosen with the origin at the center of the channel. The x-axis is parallel to the channel walls and the y-axis is perpendicular to the channel walls. The corresponding streamwise and transverse velocity components are defined as u and v, respectively. Under these assumptions, the governing equations can be expressed as follows (see e.g., [22])

$$\frac{\partial u}{\partial x}+\frac{\partial v}{\partial y}=0, \tag{2.1a}$$

$$\frac{\partial u}{\partial t}+u\frac{\partial u}{\partial x}+v\frac{\partial u}{\partial y}=-\frac{1}{\rho}\frac{\partial p}{\partial x}+\nu\left(\frac{\partial^2 u}{\partial x^2}+\frac{\partial^2 u}{\partial y^2}\right), \tag{2.1b}$$

$$\frac{\partial v}{\partial t}+u\frac{\partial v}{\partial x}+v\frac{\partial v}{\partial y}=-\frac{1}{\rho}\frac{\partial p}{\partial y}+\nu\left(\frac{\partial^2 v}{\partial x^2}+\frac{\partial^2 v}{\partial y^2}\right), \tag{2.1c}$$

where ρ, p, ν and t are the dimensional density, pressure, kinematic viscosity, and time, respectively.

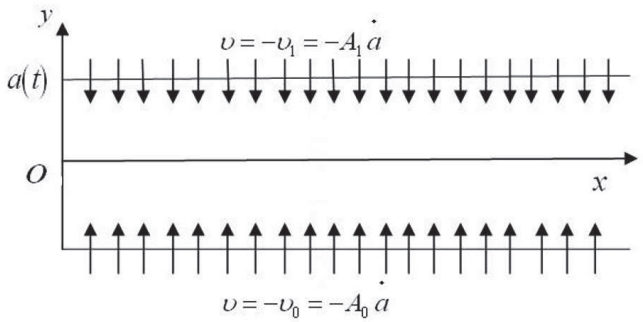

Figure 1: Two-dimensional porous channel with expanding or contracting walls.

The boundary conditions are:

$$u=0, \qquad v=-v_0=-A_0\dot{a}; \qquad y=-a(t), \tag{2.2a}$$
$$u=0, \qquad v=-v_1=-A_1\dot{a}; \qquad y=a(t), \tag{2.2b}$$
$$u=0, \qquad v=0; \qquad x=0, \tag{2.2c}$$

where $A_0=v_0/\dot{a}$, $A_1=v_1/\dot{a}$ is the measure of wall permeability. We define $A=v_0/v_1$, where $A=-1$ represent the symmetric case (that is, both walls have the equal permeability velocity). Both walls have the different permeability speed when $A\neq -1$. In the method of similarity transformation (see e.g., [16,17]), the expansion ratio $\alpha=a\dot{a}/\nu$ has to be constant. Then, the moving boundary has to be in the form of $a=a_0(1+2\nu\alpha t a_0^{-2})^{1/2}$, where a_0 denotes the initial channel location and α is the constant expansion ratio. We define the Reynolds number $R=av_1/\nu$. We will let α be the same for the purpose of comparison. But our computational method does not depend on the similarity transformation and can be used for other boundary moving functions and for variable α.

For the boundaries are moving with time, the mesh will have to change at every time step. This is not convenient and computationally costly. Thus we introduce the dimensionless variable

$$\eta=\frac{y}{a(t)}, \tag{2.3}$$

which changes the Navier-Stokes equations (2.1a)-(2.1c) to

$$\frac{\partial u}{\partial x}+\frac{1}{a(t)}\frac{\partial v}{\partial \eta}=0, \tag{2.4a}$$
$$\frac{\partial u}{\partial t}+u\frac{\partial u}{\partial x}+\frac{v}{a(t)}\frac{\partial u}{\partial \eta}=-\frac{1}{\rho}\frac{\partial p}{\partial x}+\nu\left(\frac{\partial^2 u}{\partial x^2}+\frac{1}{a^2(t)}\frac{\partial^2 u}{\partial \eta^2}\right), \tag{2.4b}$$
$$\frac{\partial v}{\partial t}+u\frac{\partial v}{\partial x}+\frac{v}{a(t)}\frac{\partial v}{\partial \eta}=-\frac{1}{\rho a(t)}\frac{\partial p}{\partial \eta}+\nu\left(\frac{\partial^2 v}{\partial x^2}+\frac{1}{a^2(t)}\frac{\partial^2 v}{\partial \eta^2}\right). \tag{2.4c}$$

The corresponding boundary conditions (2.2a)-(2.2c) become

$$u(x,\pm 1)=0, \qquad v(x,-1)=-v_0=-A_0\dot{a}, \qquad v(x,1)=-v_1=-A_1\dot{a}, \tag{2.5a}$$
$$u(0,\eta)=0, \qquad v(0,\eta)=0. \tag{2.5b}$$

We assume Neumann boundary condition for the velocity: $\partial u/\partial n=0$, $\partial v/\partial n=0$ at the outlet boundary ($x=b$).

3. Weak form and finite element scheme

3.1. Weak form

Let $\Omega\subset R^2$ be the domain of the channel. We denote by Γ the boundary of Ω. To make a weak formulation of the Eqs. (2.4a)-(2.4c), all unknown variables should be in appropriate Sobolev space. To make the problem simple we may consider u and v in V,

which is defined as $H^1(\Omega)$, and p in $L^2(\Omega)$. Furthermore, u and v satisfy conditions at boundaries where Dirichlet boundary conditions are imposed.

A weak form of the system (2.4a)-(2.4c) may be derived straightforwardly by multiplying (2.4a)-(2.4c) with test functions q, w, z respectively. Then, using integration by parts, we can obtain the weak form

$$\int_\Omega \left(\frac{\partial u}{\partial x}+\frac{1}{a(t)}\frac{\partial v}{\partial \eta}\right)q\,dx\,d\eta=0, \tag{3.1a}$$

$$\int_\Omega \left(\frac{\partial u}{\partial t}w+u\frac{\partial u}{\partial x}w+\frac{1}{a(t)}v\frac{\partial u}{\partial \eta}w+\frac{1}{\rho}\frac{\partial p}{\partial x}w +\nu\left(\frac{\partial u}{\partial x}\frac{\partial w}{\partial x}+\frac{1}{a^2(t)}\frac{\partial u}{\partial \eta}\frac{\partial w}{\partial \eta}\right)\right)dx\,d\eta=0, \tag{3.1b}$$

$$\int_\Omega \left(\frac{\partial v}{\partial t}z+u\frac{\partial v}{\partial x}z+\frac{1}{a(t)}v\frac{\partial v}{\partial \eta}z+\frac{1}{a(t)}\frac{1}{\rho}\frac{\partial p}{\partial \eta}z +\nu\left(\frac{\partial v}{\partial x}\frac{\partial z}{\partial x}+\frac{1}{a^2(t)}\frac{\partial v}{\partial \eta}\frac{\partial z}{\partial \eta}\right)\right)dx\,d\eta=0, \tag{3.1c}$$

where w, z in V, satisfying homogeneous boundary conditions at boundaries where Dirichlet boundary conditions are imposed, and q in $L^2(\Omega)$.

The divergence free condition (3.1a) is usually dealt with by a fractional step or projection method, which requests an artificial boundary condition for pressure (see e.g., [23–25]). In our paper, we shall use a penalty method or a more general sequential regularization formulation (see e.g., [24, 26–29]), where no artificial boundary condition is needed. This simplest formulation is to replace (3.1a) by the following penalized equation:

$$\int_\Omega \left(\frac{\partial u}{\partial x}+\frac{1}{a(t)}\frac{\partial v}{\partial \eta}+\varepsilon p\right)q\,dx\,d\eta=0, \tag{3.2}$$

where the small penalty constant ε is taken as $\varepsilon=10^{-7}$ in all our computations.

3.2. Finite element method

Solutions of the weak form (3.1b)-(3.2) will be numerically solved using an explicit-implicit finite difference in time and a finite element method in space. As usual, we shall use most simple continuous finite elements for the computation. The finite element space for velocity u, v is $V_h\subset V$, and the space for pressure P is $L_h\subset L^2(\Omega)$. We use the piecewise quadratic P_2 finite elements for both u and v and then the pressure p will be approximated by the piecewise linear P_1 finite element, namely, the standard Taylor-Hood finite element for the velocity-pressure variables, satisfying the inf-sup condition. We can then write the

finite element method as: find u_h, v_h in V_h, and P_h in L_h such that

$$\int_\Omega \left(\frac{\partial u_h}{\partial x} + \frac{1}{a(t)} \frac{\partial v_h}{\partial \eta} + \varepsilon p_h \right) q dx d\eta = 0, \tag{3.3a}$$

$$\int_\Omega \left(\frac{\partial u_h}{\partial t} w + u_h \frac{\partial u_h}{\partial x} w + \frac{1}{a(t)} v_h \frac{\partial u_h}{\partial \eta} w + \frac{1}{\rho} \frac{\partial p_h}{\partial x} w + \nu \left(\frac{\partial u_h}{\partial x} \frac{\partial w}{\partial x} + \frac{1}{a^2(t)} \frac{\partial u_h}{\partial \eta} \frac{\partial w}{\partial \eta} \right) \right) dx d\eta = 0, \tag{3.3b}$$

$$\int_\Omega \left(\frac{\partial v_h}{\partial t} z + u_h \frac{\partial v_h}{\partial x} z + \frac{1}{a(t)} v_h \frac{\partial v_h}{\partial \eta} + \frac{1}{a(t)} \frac{1}{\rho} \frac{\partial p_h}{\partial \eta} z + \nu \left(\frac{\partial v_h}{\partial x} \frac{\partial z}{\partial x} + \frac{1}{a^2(t)} \frac{\partial v_h}{\partial \eta} \frac{\partial z}{\partial \eta} \right) \right) dx d\eta = 0, \tag{3.3c}$$

for all w, z in V_h, which is the subspace of the Sobolev space $H^1(\Omega)$ of zero trace functions on boundaries where Dirichlet boundary conditions are imposed and all q in L_h.

We define $H_h = V_h \times V_h \times L_h$, $\delta t > 0$ to be the size of the time step, and $(u_h^n, v_h^n, p_h^n) \in H_h$ to be an approximation of $u(t^n) = u(n\delta t)$, $v(t^n) = v(n\delta t)$ and $p(t^n) = p(n\delta t)$. The approximation solution at time $t^{n+1} = (n+1)\delta t$ denoted as $(u_h^{n+1}, v_h^{n+1}, p_h^{n+1}) \in H_h$ is obtained by the following typical temporal scheme:

$$\int_\Omega \left(\frac{\partial u_h^{n+1}}{\partial x} + \frac{1}{a(t^{n+1})} \frac{\partial v_h^{n+1}}{\partial \eta} + \varepsilon p_h^{n+1} \right) q dx d\eta = 0, \tag{3.4a}$$

$$\int_\Omega \left(\frac{u_h^{n+1} - u_h^n}{\delta t} w + u_h^n \frac{\partial u_h^n}{\partial x} w + \frac{1}{a(t^n)} v_h^n \frac{\partial u_h^n}{\partial \eta} w + \frac{1}{\rho} \frac{\partial p_h^{n+1}}{\partial x} w + \nu \left(\frac{\partial u_h^{n+1}}{\partial x} \frac{\partial w}{\partial x} + \frac{1}{a^2(t^{n+1})} \frac{\partial u_h^{n+1}}{\partial \eta} \frac{\partial w}{\partial \eta} \right) \right) dx d\eta = 0, \tag{3.4b}$$

$$\int_\Omega \left(\frac{v_h^{n+1} - v_h^n}{\delta t} z + u_h^n \frac{\partial v_h^n}{\partial x} z + \frac{1}{a(t^n)} v_h^n \frac{\partial v_h^n}{\partial \eta} z + \frac{1}{a(t^{n+1})} \frac{1}{\rho} \frac{\partial p_h^{n+1}}{\partial \eta} z + \nu \left(\frac{\partial v_h^{n+1}}{\partial x} \frac{\partial z}{\partial x} + \frac{1}{a^2(t^{n+1})} \frac{\partial v_h^{n+1}}{\partial \eta} \frac{\partial z}{\partial \eta} \right) \right) dx d\eta = 0, \tag{3.4c}$$

for all $(q, w, z) \in H_h$, satisfying zero boundary conditions at the boundaries where Dirichlet boundary conditions are imposed.

4. Computational multiple solutions for symmetric and asymmetric flows

Now for the symmetric flow (i.e., $A = -1$), we are using the finite element methods proposed in Section 3 to solve the Navier-Stokes equations (2.1a)-(2.1c) directly and our code is written with the help of the software FreeFem++ and MATLAB. The symmetric flow was studied in Xu et al. [17] with the similarity transformation and the HAM. For

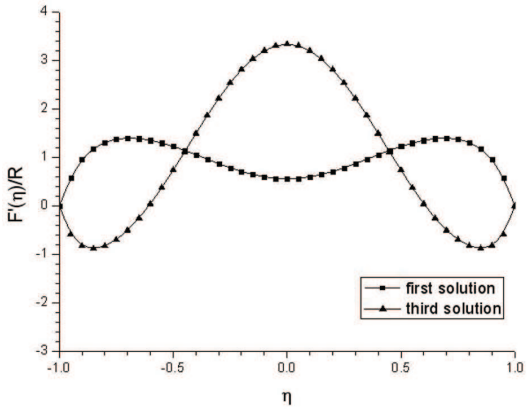

Figure 2: Numerical solutions at $x = 2$ for $F'(\eta)/R$ in case of $R = -10$ and $\alpha = 4$.

the comparison purpose we will use the boundary moving function $a(t)$ given in [17] (see our description in Section 2). We will first compare our numerical solutions with those obtained by the HAM in [17] so as to validate our computational method and code. In addition, through the dynamic solving process we justify the stability of those solutions as well.

We first give computational results for a few different values of R and α. To see details of the velocity field we use a 100×40 grid which triangulates the rectangular domain into a triangular mesh with 4141 nodes and 8000 elements. The time step $\Delta t = 0.0001$ and the kinematic viscosity $\nu = 0.01$ are considered here. The solutions are all shown at $x = 2$.

As shown in Fig. 2, two solutions are obtained at $R = -10$ and $\alpha = 4$ using the finite element method. We can relatively easily calculate the first solution in [17] and another solution (we call it the third solution, which was not found in [17]) at $t = 0.1$, 0.2, 0.3, respectively. We do not observe any significant difference at $t = 0.1$, 0.2, 0.3. This indicates that the two solutions have already stably reached the steady state. The solutions at $t = 0.3$ are depicted in Fig. 2. However, it is difficult for us to find the second solution shown in [17]. Even if we start from a very small perturbation of the second solution given in [17] we observe that the numerical solution stay near the second solution at a very short time (e.g., $t = 0.01$), but as the time increases, the solution quickly becomes large. This computational result may suggest that the second solution obtained in [17] is physically unstable.

In Fig. 3, two distinct solutions are shown in the case of $R = -11$ and $\alpha = 3/2$. Again the first solution given in [17], just as the second solution in the case of $R = -10$ and $\alpha = 4$, can blow up quickly. The second and the third solutions can be obtained by our direct computational method, so they are both stable solutions. They are shown in Fig. 3 at times $t = 0.4$ and $t = 0.1$, when they reach the steady state, respectively.

In Fig. 4, both type I and type II solutions given in [17] can be obtained at $R = -20$ and $\alpha = 1$ with the time $t = 0.3$. But we cannot find the type III solution. Even if we start from a perturbation of the type III solution, it quickly becomes large. A possible reason is again that the type III solution may be physically unstable. The velocity fields of type I and

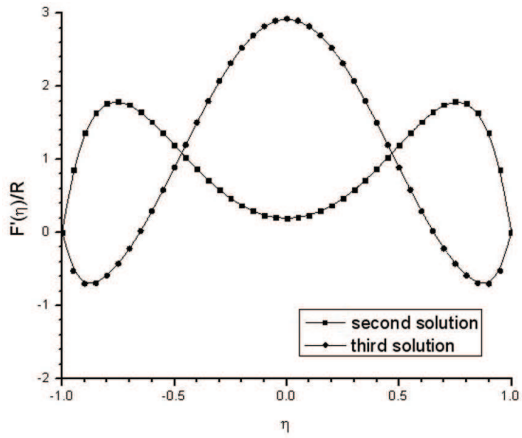

Figure 3: Numerical solutions at $x = 2$ for $F'(\eta)/R$ in case of $R = -11$ and $\alpha = 3/2$.

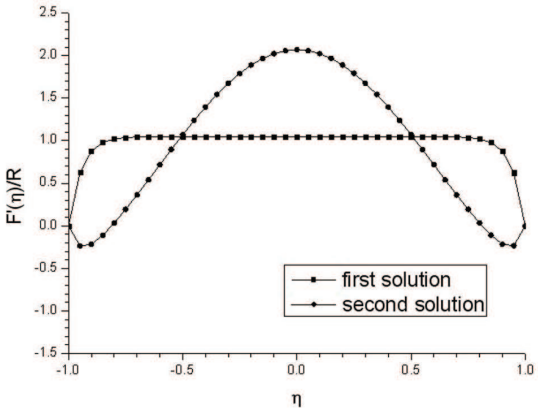

Figure 4: Numerical solutions at $x = 2$ for $F'(\eta)/R$ in case of $R = -20$ and $\alpha = 1$.

type II solutions in the whole channel are depicted in Figs. 6 and 7, respectively.

As Fig. 5 indicated, we also obtain dual solutions in the case of $R = -8$, $\alpha = 3$ numerically, which was not included in the range discussed in Xu et al. [17]. The two solutions are depicted at the time $t = 0.2$.

The numerical solutions of $F'(0)/R$ are compared with the HAM approximations in the case of $R = -10$, $\alpha = 4$ and $R = -11$, $\alpha = 3/2$ just as listed in Table 1. We observe that

Table 1: Comparison of numerical and analytical results as $R = -10$, $\alpha = 4$ and $R = -11$, $\alpha = 3/2$.

	$F'(0)/R$	Numerical solutions	Analytical solutions
$R = -10$, $\alpha = 4$	First solution	0.561771	0.624967
	Third solution	3.343143	not available
$R = -11$, $\alpha = \frac{3}{2}$	Second solution	0.193505	0.169378
	Third solution	2.922919	2.76218

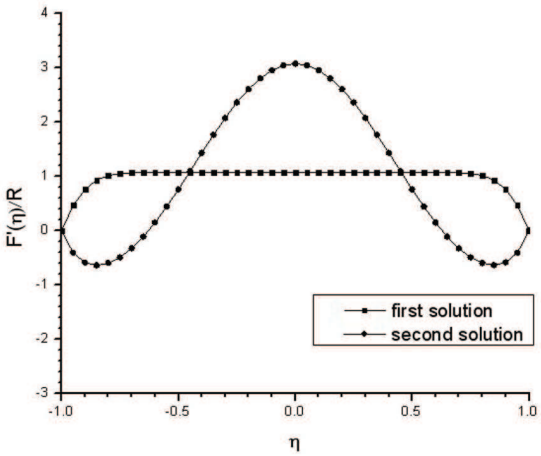

Figure 5: Numerical solutions at $x = 2$ for $F'(\eta)/R$ in case of $R = -8$ and $\alpha = 3$.

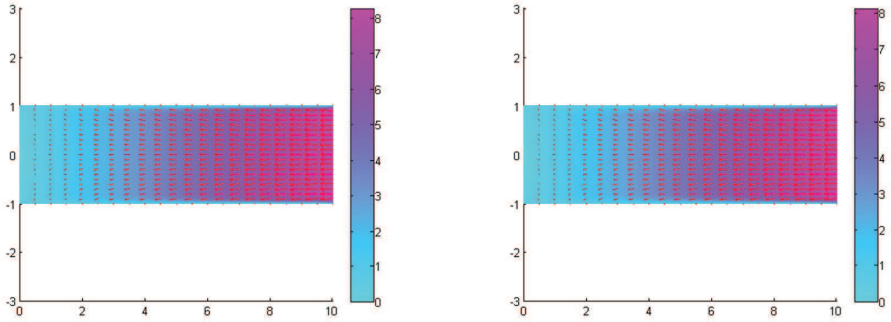

(a) $t = 0.1$ (b) $t = 0.3$

Figure 6: The velocity field of the first solution in the $R = -20$, $\alpha = 1$ case.

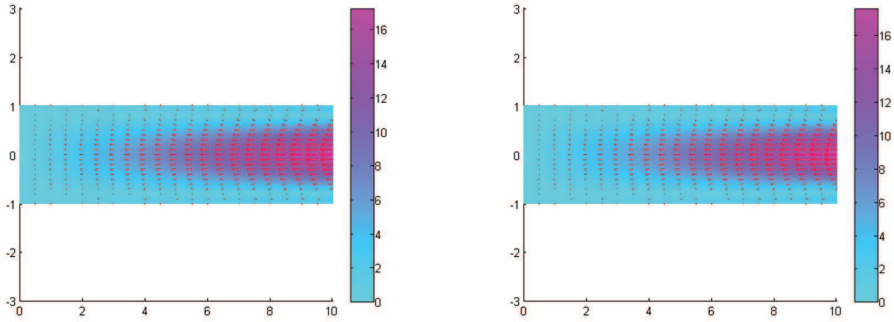

(a) $t = 0.1$ (b) $t = 0.3$

Figure 7: The velocity field of the second solution in the $R = -20$, $\alpha = 1$ case.

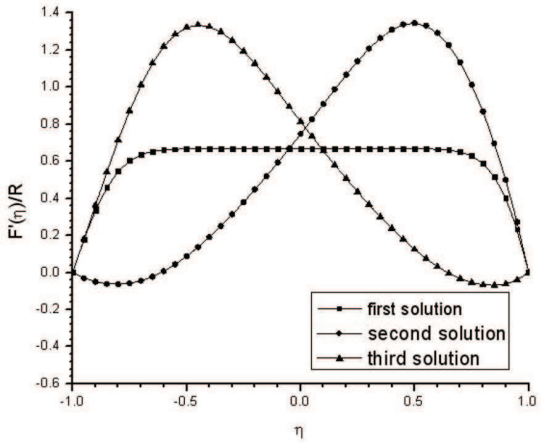

Figure 8: Numerical solutions at $x = 2$ for $F'(\eta)/R$ at $R = -5$, $\alpha = 1$ when $A = -0.2$.

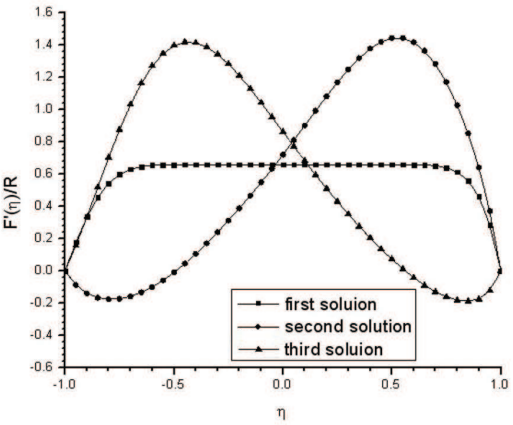

Figure 9: Numerical solutions at $x = 2$ for $F'(\eta)/R$ at $R = -10$, $\alpha = 4$ when $A = -0.2$.

our numerical solutions and the analytical approximations are pretty close.

Next we seek possible multiple solutions for the asymmetrical flow (i.e., different permeability speed on the upper and lower walls), where no analysis has been available through the similarity transformation and the HAM. We have obtained dual solutions earlier for some R and α in the symmetric case (i.e., $A = -1$) using our finite element method. Now for the asymmetric case, e.g., $A = -0.2$ (that is, the suction velocity at the lower wall is 20% of that at the upper wall), we can find three stable solutions for three cases ($R = -5$ and $\alpha = 1$, $R = -10$ and $\alpha = 4$, $R = -12$ and $\alpha = 2$) numerically using the same finite element method. We also choose a 100×40 grid, the time step $\Delta t = 0.0001$ and the kinematic viscosity $\nu = 0.01$ in the program. We calculate each solution at $t = 0.1$, 0.2, 0.3, respectively. Multiple solutions in Figs. 8-10 are all shown at $t = 0.3$. Figs. 11-19 depict velocity fields for all solutions of all three cases.

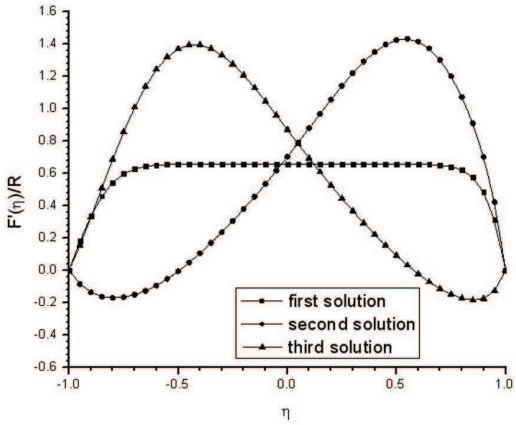

Figure 10: Numerical solutions at $x = 2$ for $F'(\eta)/R$ at $R = -12$, $\alpha = 2$ when $A = -0.2$.

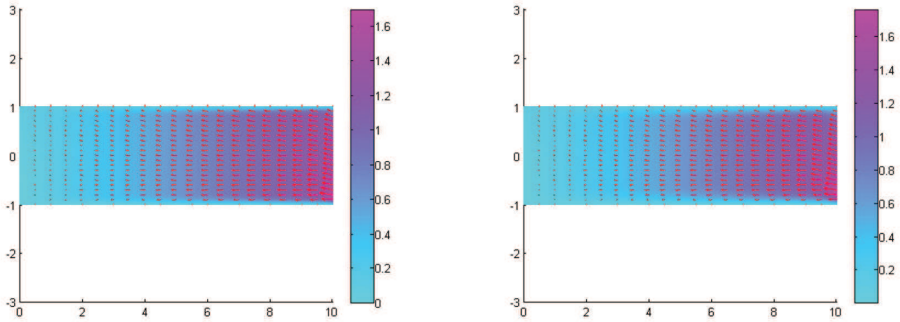

(a) $t = 0.1$ (b) $t = 0.3$

Figure 11: The velocity field of the first solution at $R = -5$, $\alpha = 1$ when $A = -0.2$.

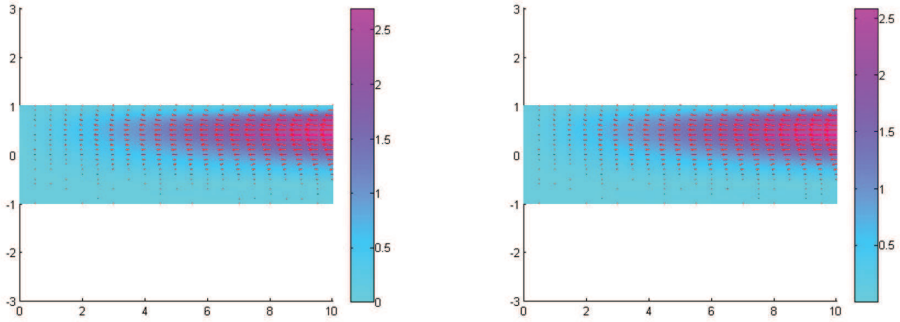

(a) $t = 0.1$ (b) $t = 0.3$

Figure 12: The velocity field of the second solution at $R = -5$, $\alpha = 1$ when $A = -0.2$.

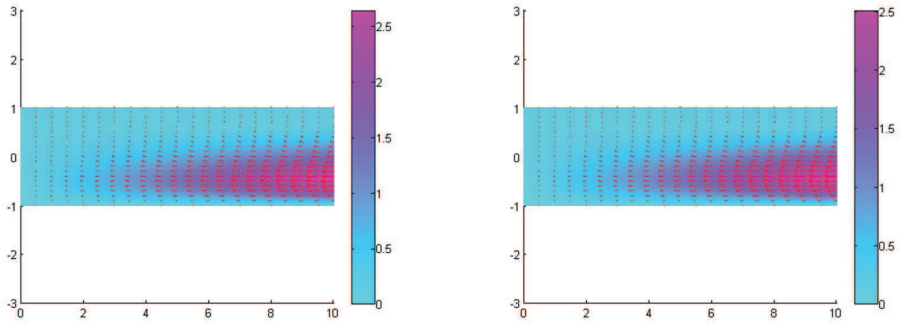

(a) $t = 0.1$ (b) $t = 0.3$

Figure 13: The velocity field of the third solution at $R = -5$, $\alpha = 1$ when $A = -0.2$.

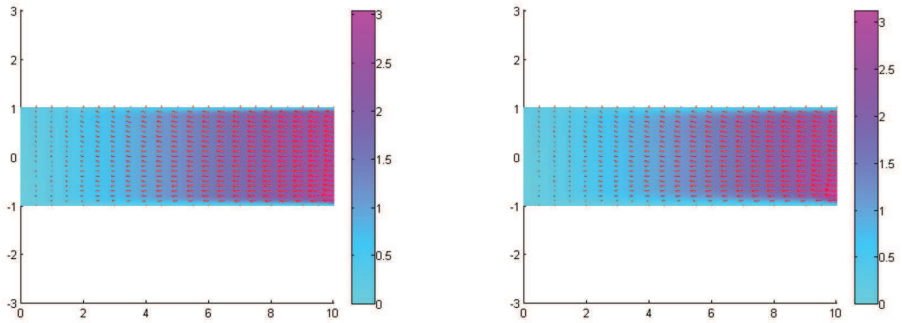

(a) $t = 0.1$ (b) $t = 0.3$

Figure 14: The velocity field of the first solution at $R = -10$, $\alpha = 4$ when $A = -0.2$.

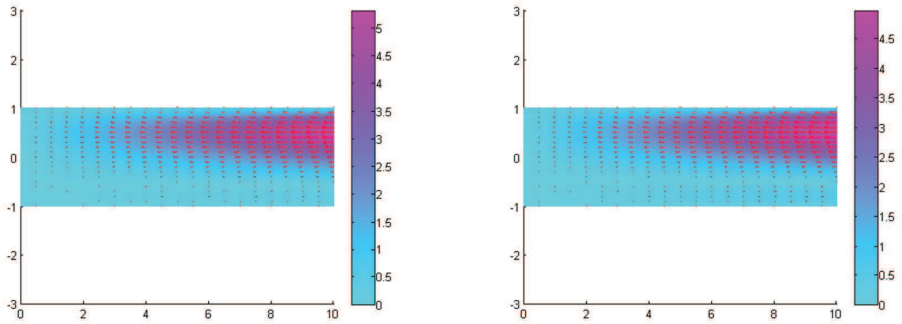

(a) $t = 0.1$ (b) $t = 0.3$

Figure 15: The velocity field of the second solution at $R = -10$, $\alpha = 4$ when $A = -0.2$.

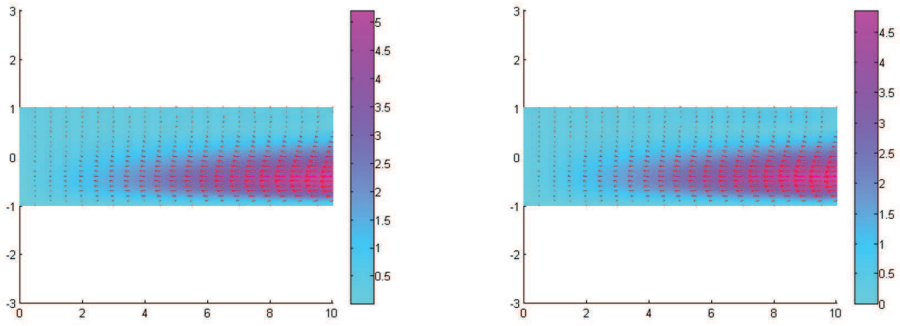

(a) $t = 0.1$ (b) $t = 0.3$

Figure 16: The velocity field of the third solution at $R = -10$, $\alpha = 4$ when $A = -0.2$.

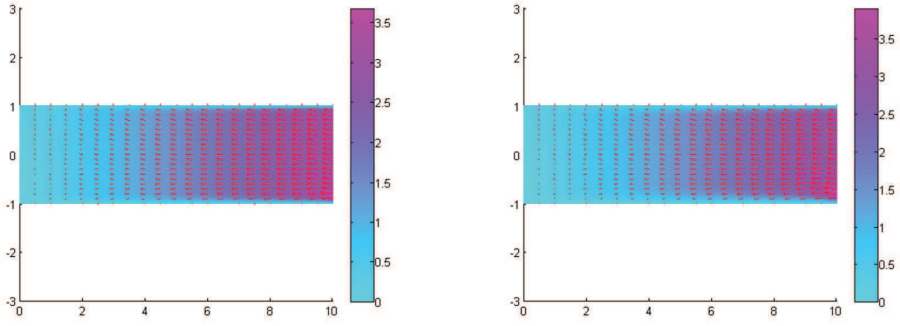

(a) $t = 0.1$ (b) $t = 0.3$

Figure 17: The velocity field of the first solution at $R = -12$, $\alpha = 2$ when $A = -0.2$.

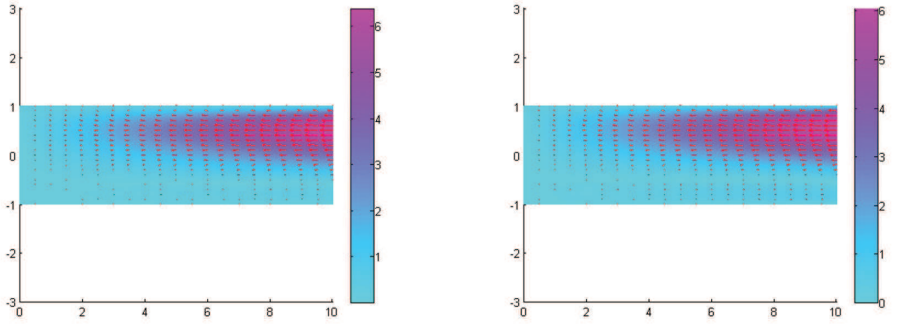

(a) $t = 0.1$ (b) $t = 0.3$

Figure 18: The velocity field of the second solution at $R = -12$, $\alpha = 2$ when $A = -0.2$.

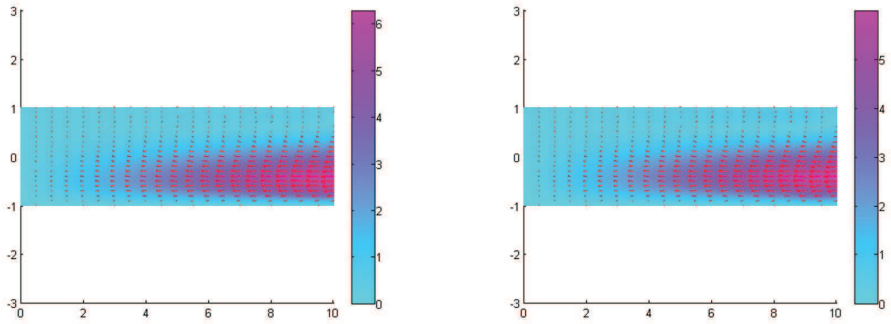

(a) $t = 0.1$ (b) $t = 0.3$

Figure 19: The velocity field of the third solution at $R = -12$, $\alpha = 2$ when $A = -0.2$.

5. Conclusions

This paper has proposed an efficient explicit-implicit finite element scheme to find numerical solutions of the governing Navier-Stokes equations with moving porous walls directly. For the suction driven channel, we obtained multiple solutions with several R and α using the method for the symmetric flow and the asymmetric flow. It is shown that dual or three solutions exist for the different values of R and α. The numerical solutions for the symmetric flow we obtained match well with some obtained by the similarity transformation and HAM approximations. In some cases, we cannot obtain three solutions predicted by the similarity transformation and HAM (For example, the second solution in case of $R = -10$, $\alpha = 4$ and the type III solution at $R = -20$, $\alpha = 1$). This indicates that one of these three solutions obtained through similarity transformation may be unstable in time. Finally, we have also considered three cases where the permeability velocities are asymmetric at the upper and lower walls. There is no study of multiple solutions for these cases using similarity transformation and HAM. Using our finite element method we find that three solutions also exist for some choices of R and α in the case of the asymmetric flow.

Acknowledgments The work is supported by the Research Foundation of Engineering Research Institute of USTB (No. Yj2011-015), the Fundamental Research Funds for the Central Universities (No. FRF-TP-12-108A, No.06108137), University of Science and Technology Beijing Research Grant (No. 06108038) and the national natural Science Foundations of China (Nos. 51174028, 51004013).

References

[1] A. S. Berman, *Laminar flow in channels with porous walls*, J. Appl. Phys., 24 (1953), pp. 1232–1235.

[2] S. W. Yuan, *Further investigations of laminar flow in channels with porous walls*, J. Appl. Phys., 27 (1956), pp. 267–269.

[3] R. M. Terrill and G. M. Shrestha, *Laminar flow through parallel and uniformly porous walls of different permeability*, ZAMP, 16 (1965), pp. 471–482.
[4] U. Suryaprakasarao, *Flow in channels with porous walls in the presence of a transverse magnetic field*, Appl. Sci. Res., 9 (1961), pp. 374–382.
[5] R. M. Terrill, *Laminar flow in a uniformly porous channel*, The Aeronautical Quarterly, XV (1964), pp. 299–310.
[6] R. M. Terrill, *Laminar flow in a uniformly porous channel with large injection*, The Aeronautical Quarterly, 16 (1965), pp. 323–332.
[7] W. A. Robinson, *The existence of multiple solutions for the laminar flow in a uniformly porous channel with suction at both walls*, J. Eng. Math., 10 (1976), pp. 23–40.
[8] C. Lu,A. D. Macjillvary and S. P. Hastings, *Asymptotic behaviour of solutions of a similarity equation for laminar flows in channels with porous walls*, IMA. J. Appl. Math., 49 (1992), pp. 139–162.
[9] M. B. Zaturska,P. G. Drazin and W. H. H. Banks, *On the flow of a viscous fluid driven along a channel by suction at porous walls*, Fluid Dyn. Res., 4 (1988), pp. 151–178.
[10] J. Majdalani and C. Zhou, *Moderate-to-large injection and suction driven channel flows with expanding or contracting walls*, ZAMM. Z. Angew. Math. Mech., 83 (2003), pp. 181–196.
[11] J. Majdalani and C. Zhou, *Large injection and suction driven channel flows with expanding and contracting walls*, 31st AIAA Fluid Dynamics Conference 11-14 June 2001 Anaheim, CA.
[12] J. Majdalani and C. Zhou, *Inner and outer solutions for the injection driven channel flows with retractable walls*, 33st AIAA Fluid Dynamics Conference 23-26 June 2003 Orlando, FL.
[13] J. Majdalani,C. Zhou and C. A. Dawson, *Two dimensional viscous flow between slowly expanding or contracting walls with weak permeability*, J. Biomech., 35 (2002), pp. 1399–1403.
[14] S. Asghar,M. Mushtap and T. Hayat, *Flow in a slowing deforming channel with weak permeability: an analytical approach*, Nonlinear Anal. Real., 11 (2010), pp. 555–561.
[15] D. Saeed, M. R. Mohammad and D. Ahmad, *Analytical approximate solutions for two dimensional viscous flow through expanding or contracting gaps with permeable walls*, Centr. Euro. J. Phys., 7 (2009), pp. 791–799.
[16] E. C. Dauenhauer and J. Majdalani, *Exact self-similarity solution of the Navier-Stokes equations for a porous channel with orthogonally moving walls*, Phys. Fluids, 15 (2003), pp. 1485–1495.
[17] H. Xu, Z. L. Lin, S. J. Liao, J. Z. Wu and J. Majdalani, *Homotopy based solutions of the Navier-Stokes equations for a porous channel with orthogonally moving walls*, Phys. Fluids, 22 (2010), 053601.
[18] L. Durlofsky and J. F. Brady, *The spatial stability of a class of similarity solutions*, Phys. Fluids, 27 (1984), pp. 1068–1076.
[19] R. Glowinski, Finite Element Methods for Incompressible Viscous Flow, In Handbook of Numerical Analysis, IX, P. G. Ciarlet and J.-L. Lions eds., North-Holland, Amsterdam, 2003, pp. 3–1176.
[20] R. Teman, Navier-Stokes Equations: Theory and Numerical Analysis, North-Holland, 1997.
[21] L. Quartapelle, Numerical Solution of the Incompressible Navier-Stokes Equations, International Series of Numerical Mathematics, 113, Brikhauser, 1993.
[22] X. H. Si, L. C. Zheng, X. X. Zhang and Y. C, *Homotopy analysis solutions for the asymmetric laminar flow in a porous channel with expanding or contracting walls*, Acta Mech. Sinica, 27 (2011), pp. 208–214.
[23] P. M. Gresho, *Incompressible fluid dynamics: some fundamental formulation issues*, Annu. Rev. Fluid Mech., 23 (1991), pp. 413–453.
[24] P. Lin, *A sequential regularization method for time-dependent incompressible Navier-Stokes*

equations, SIAM J. Numer. Anal., 34(3) (1997), pp. 1051–1071.
[25] D. Rempfer, *On boundary conditions for incompressible Navier-Stokes problems*, Appl. Mech. Rev., 59 (2006), pp. 107–125.
[26] P. Lin, X. Q. Chen and M. T. Ong, *Finite element methods based on a new formulation for the non-stationary incompressible Navier-Stokes equations*, Int. J. Numer. Mech. Fluids, 46 (2004), pp. 1169–1180.
[27] P. Lin and C. Liu, *Simulations of singularity dynamics in liquid crystal flows: a finite element approach*, J. Comput. Phys., 215 (2006), pp. 348–362.
[28] X. L. Lu, P. Lin and J. G. Liu, *Analysis of a sequential regularization method for the unsteady Navier-Stokes equations*, Math. Comput., 77(263) (2008), pp. 1467–1494.
[29] H. D. Shi, P. Lin, B. T. Li and L. C. Zheng, *A finite element method for heat transfer of power-law flow in channels with a transverse magnetic field*, 2011, submitted.